Biocompatible inorganic nanoparticles for [^{18}F]-fluoride binding with applications in PET imaging

ELECTRONIC SUPPLEMENTARY INFORMATION

Maite Jauregui-Osoro,[1] Peter A Williamson,[1] Arnaud Glaria,[1] Kavitha Sunassee,[1] Putthiporn Charoenphun,[1] Mark A Green[2] and Philip J Blower[1]*

[1]Division of Imaging Sciences, King's College London, St. Thomas' Hospital, London SE1 7EH, UK

[2]Department of Physics, King's College London, The Strand, London WC2R 2LS

Fig. S1: X-ray powder diffractogram of HA1, HA2, HA3 and HA4

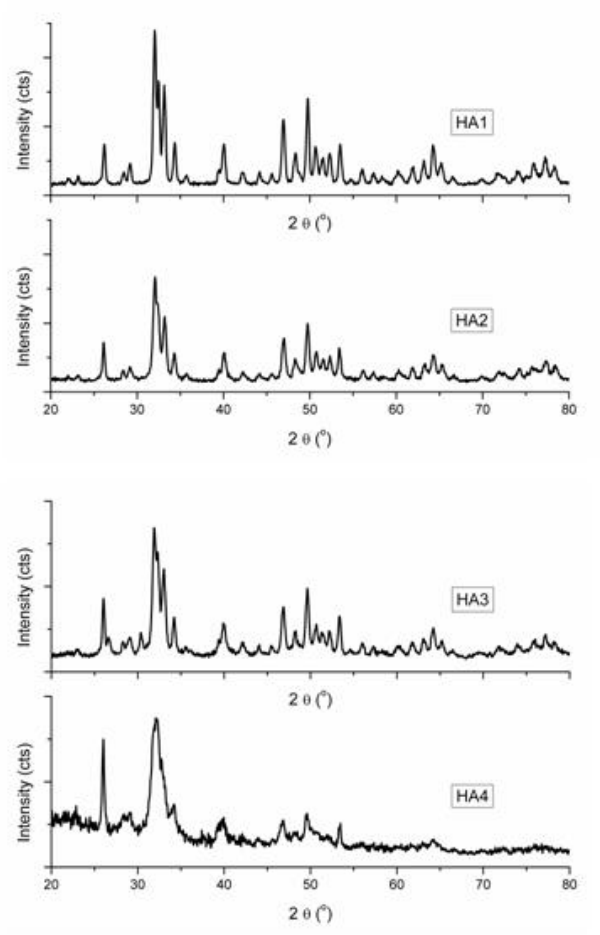

Fig. S2: Infrared spectra of HA1, HA2, HA3, HA4 and HA4-PEG

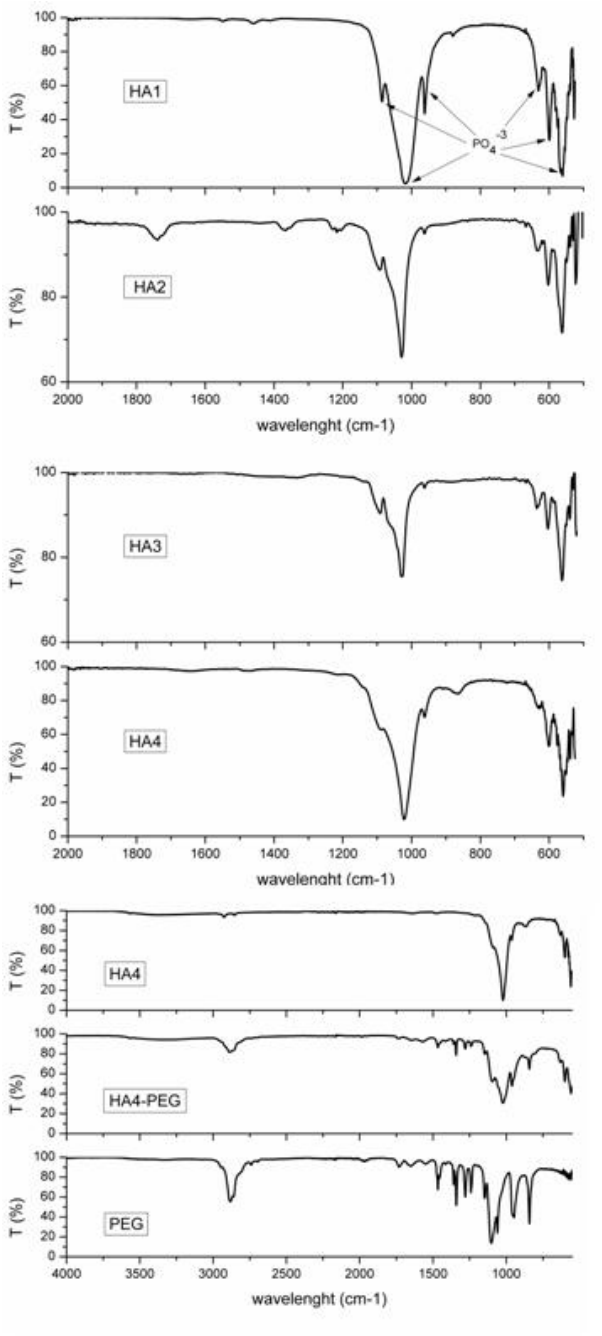

Fig. S3: X-ray powder diffractogram of Mes-SiO_2

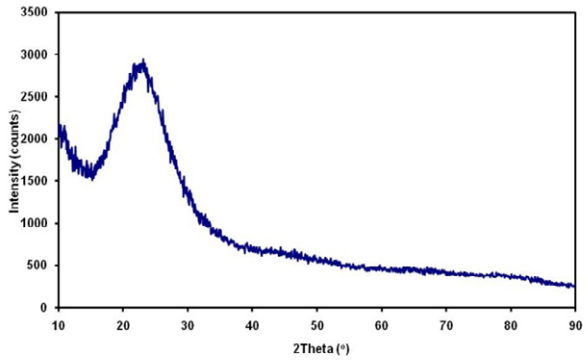

Fig. S4: Infrared spectra of Mes-SiO_2 NPs (before and after washing) and CTAC.

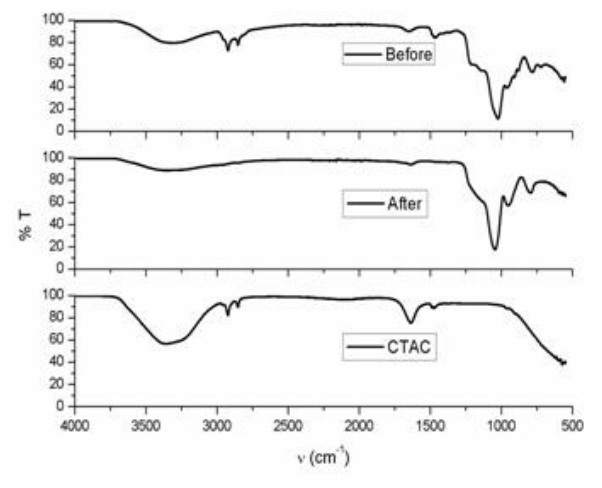

Fig. S5: Dynamic Light Scattering (DLS) of the nanoparticles solutions at a concentration of 1 mg/mL for Alhydrogel^{TM}, HA4, HA4Ale, HA4PEG and 0.2 mg/ml for HA1, HA2 and HA3.

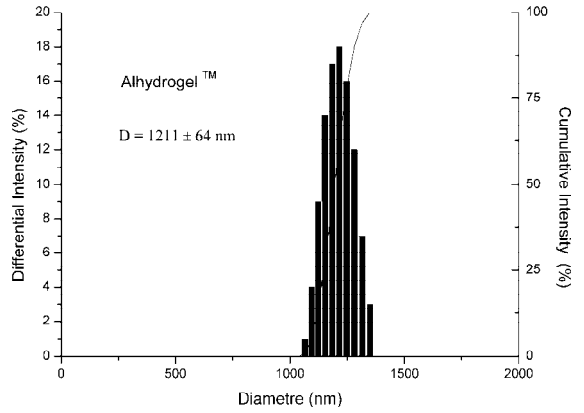

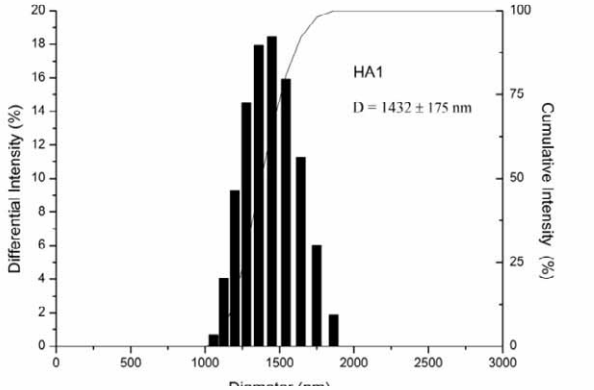

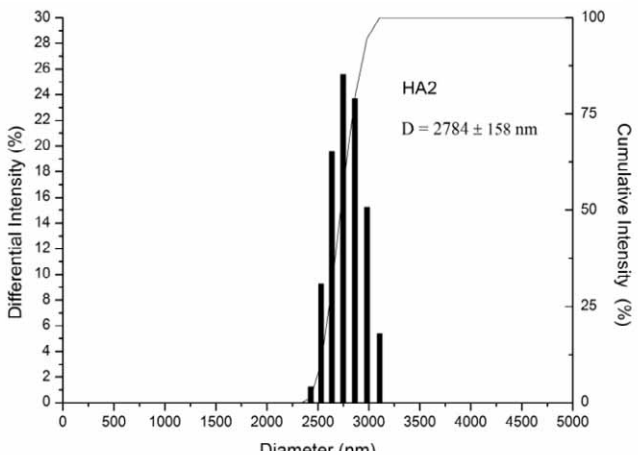

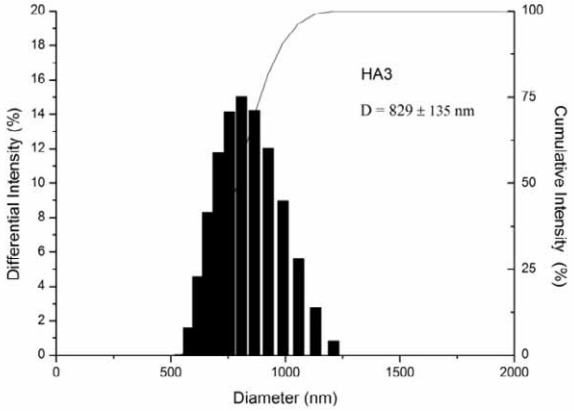

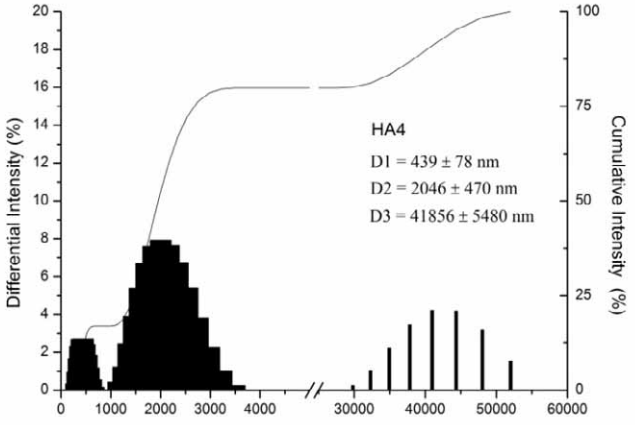

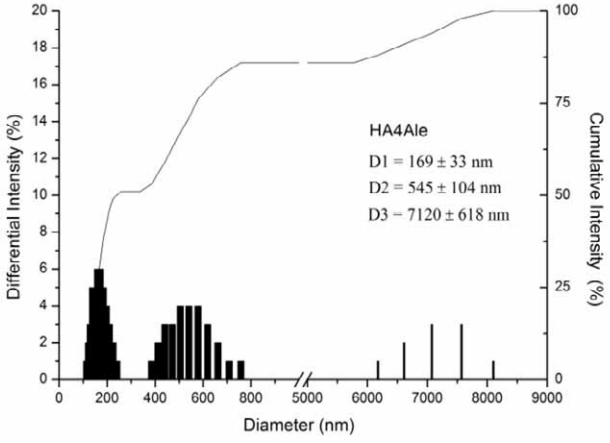

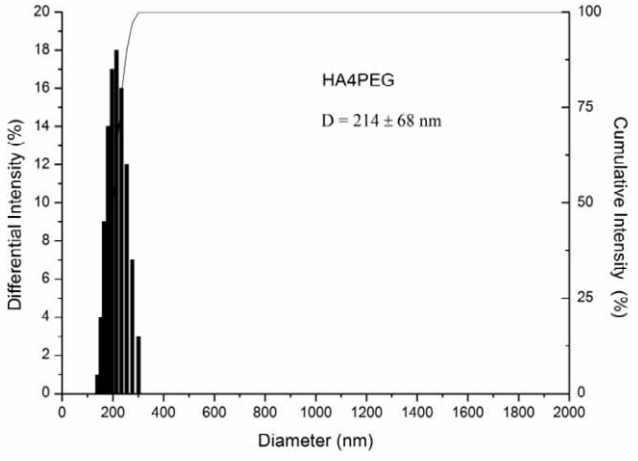

Fig. S6: [^{18}F] Fluoride binding to HA2, and HA3 in different media (water, Tris, PBS and cell medium).

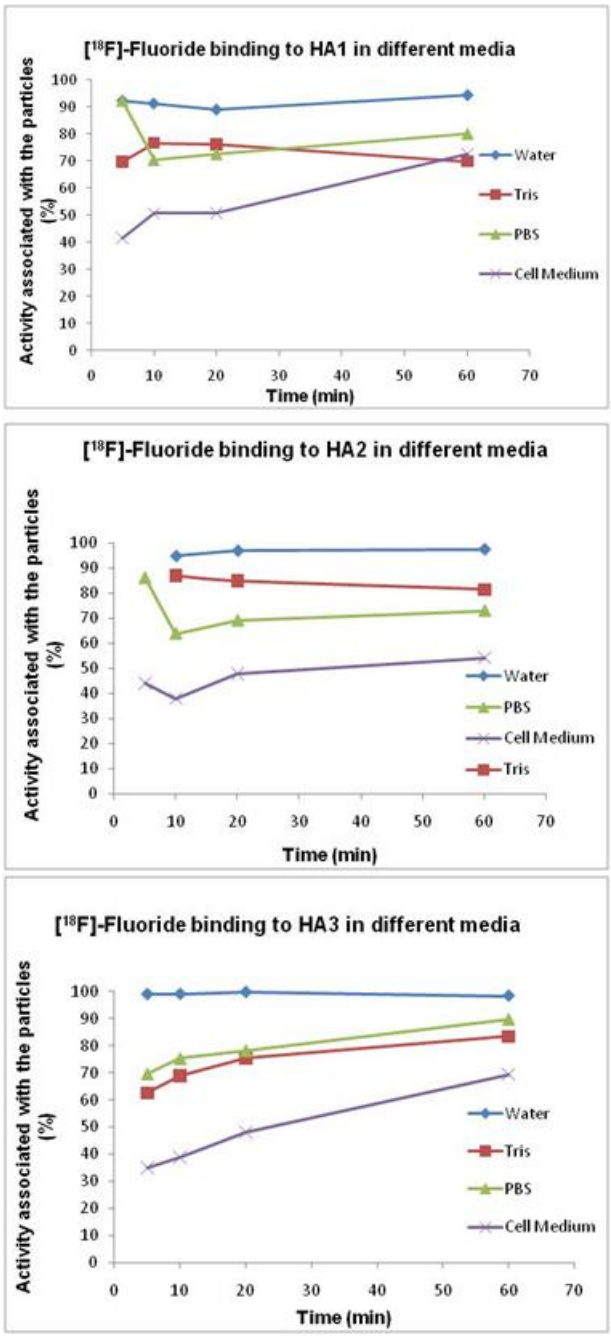

Table S1: Effect of competing substances on binding of [^{18}F]-fluoride to hydroxyapatite HA4 and $Al(OH)_3$. HMP is sodium hexametaphosphate; BP is the bisphosphonate Alendronate; CTAB is cetyltrimethylammonium bromide; phosphate is phosphate buffered saline.

Material	Inhibitor	Log [Inhibitor]	%binding	Stdev
HA4	NaCl	0	79.1	2.1
HA4	NaCl	-0.3	79.7	2.2
HA4	NaCl	-1	78.1	4.6
HA4	HMP	-1	18.3	1.7
HA4	HMP	-2	19.1	0.3
HA4	HMP	-3	49.9	0.8
HA4	HMP	-4	87.8	0.2
HA4	HMP	-5	88.9	0.4
HA4	Citrate	-1	57.4	0.3
HA4	Citrate	-2	72.7	0.2
HA4	Citrate	-3	88.5	0.3
HA4	Citrate	-4	93.1	0.6
HA4	Citrate	-5	93.2	0.4
HA4	BP	-2	78.7	0.6
HA4	BP	-3	80.6	0.2
HA4	BP	-4	87.4	0.6
HA4	BP	-5	85.8	0.5
HA4	BP	-6	92.7	0.9
HA4	BP	-7	93.3	0.7
HA4	CTAB	-1	93.2	0.2
HA4	CTAB	-2	88.6	2.8
HA4	CTAB	-3	91.1	1.8
HA4	CTAB	-4	88.7	2.7
HA4	CTAB	-5	88.9	1.9
HA4	Tris	-1	62.82	0.4
HA4	phosphate	-1	92.39	0.7
Al(OH)3	NaCl	0	98.6	0.8
Al(OH)3	NaCl	-0.3	97.8	0.6
Al(OH)3	NaCl	-1	98.5	0.1
Al(OH)3	HMP	-1	7.5	1.6
Al(OH)3	HMP	-2	8.7	0.3
Al(OH)3	HMP	-3	77.2	0.5
Al(OH)3	HMP	-4	89.8	0.4
Al(OH)3	Citrate	-1	10.4	0.7
Al(OH)3	Citrate	-2	20.1	0.8
Al(OH)3	Citrate	-3	39.5	0.9
Al(OH)3	Citrate	-4	87.4	0.5
Al(OH)3	Citrate	-5	90.2	0.5
Al(OH)3	BP	-1	68.8	0.3
Al(OH)3	BP	-2	69.4	0.5
Al(OH)3	BP	-3	80.5	1.2
Al(OH)3	BP	-4	86.8	1.6

Al(OH)3	BP	-5	88.0	1.1

Fig. S7: Effect of carrier fluoride concentration on binding of [^{18}F]-fluoride to HA2

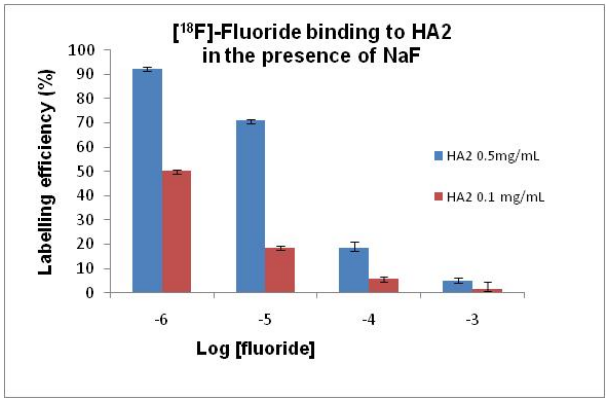

Fig. S8: Kinetic stability of [^{18}F]-HA4 and $Al(OH)_3$ in the presence of NaF and alendronate

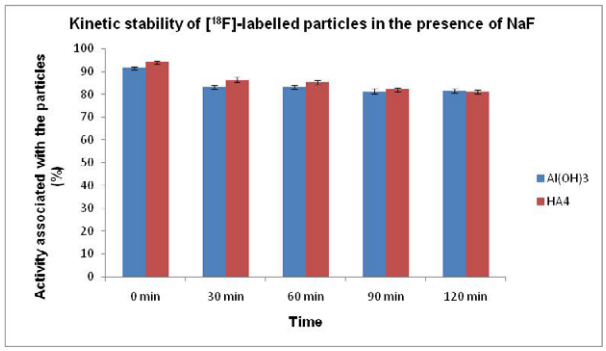

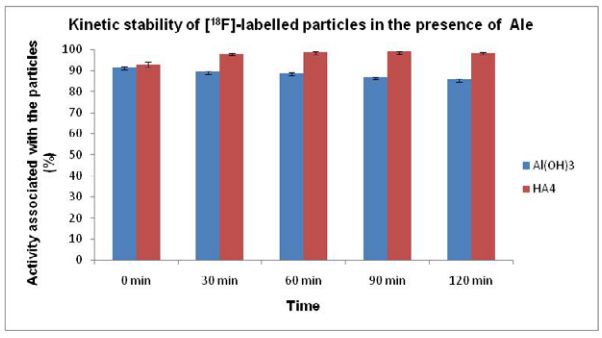

Fig. S9. Transmission electron micrograph of macrophages after incubation with $Al(OH)_3$ showing particles sequestered within phagosomes. The right image is close-up of the top right region of the left.

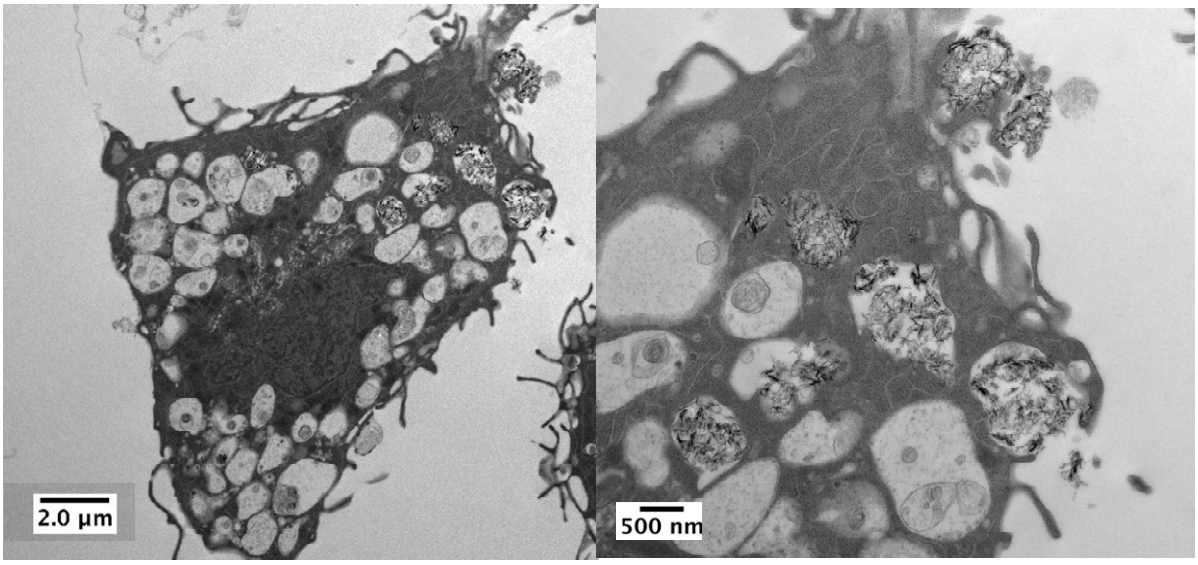

Fig S10: Biodistribution of [^{18}F]-HA2, HA4, HA4-PEG and $Al(OH)_3$ after subcutaneous (s.c.) and intramuscular (i.m.) injections and intravenous (i.v.) injection in BALB/c mice.

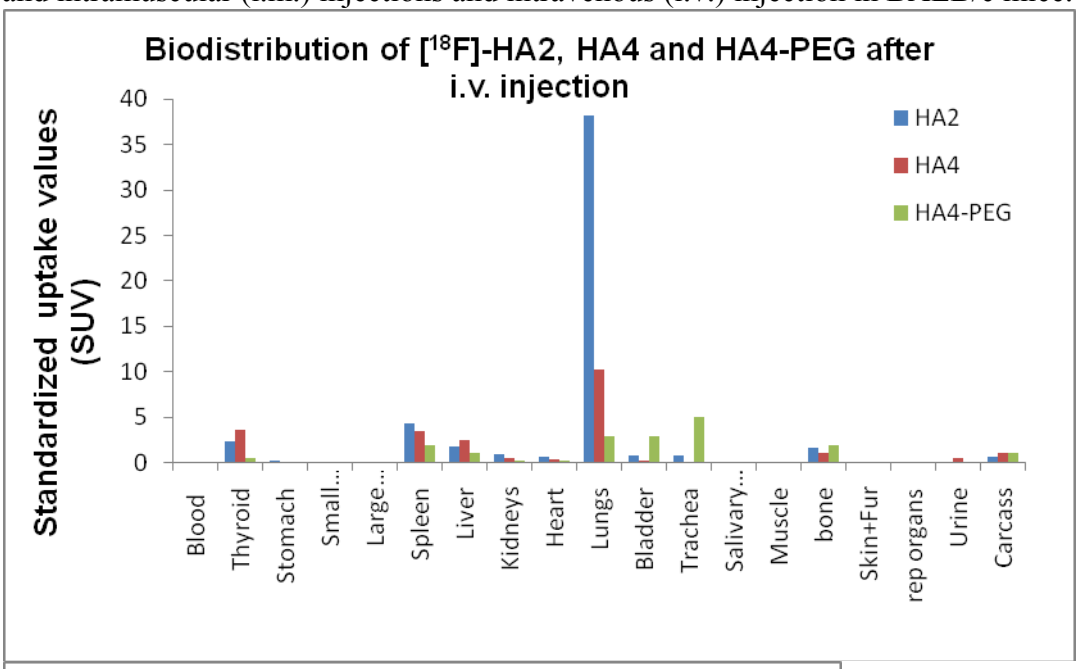

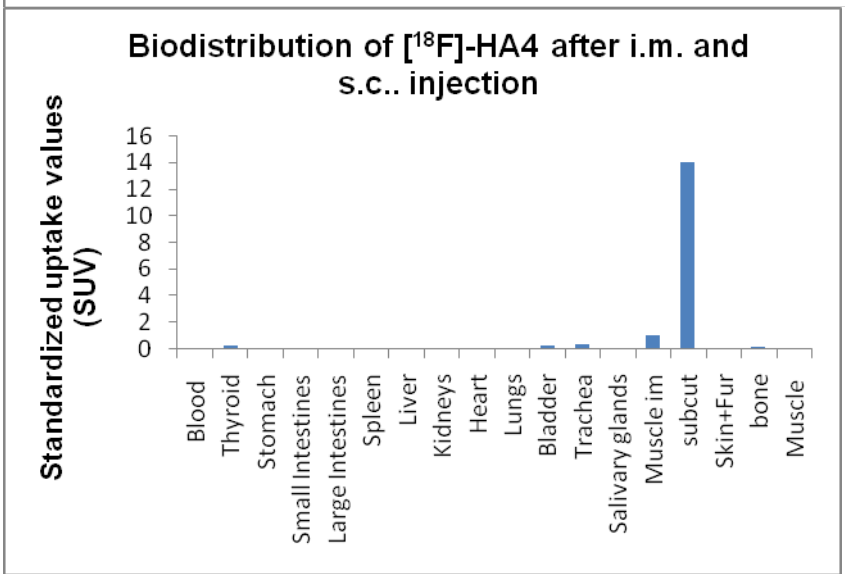

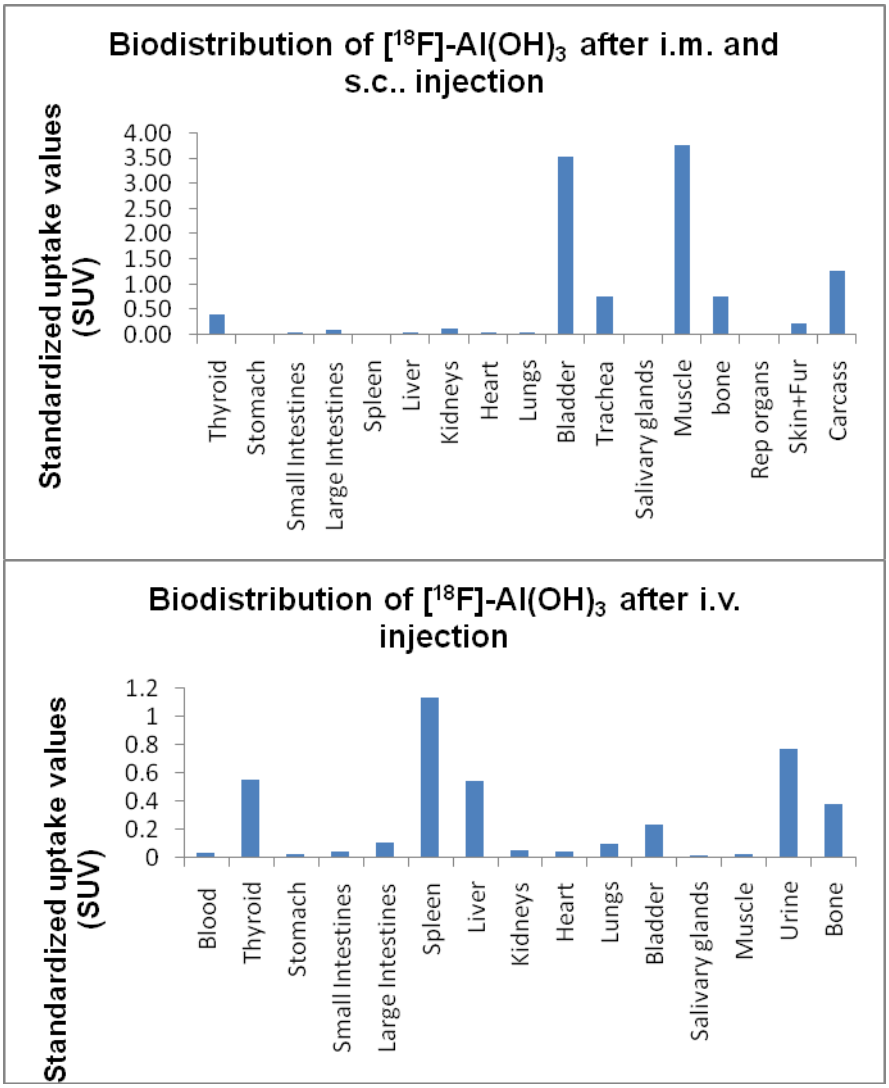
Biodistribution of [18F]-Al(OH)3 after i.m. and s.c.. injection
Standardized uptake values (SUV)
4.00
3.50
3.00
2.50
2.00
1.50
1.00
0.50
0.00
Thyroid
Stomach
Small Intestines
Large Intestines
Spleen
Liver
Kidneys
Heart
Lungs
Bladder
Trachea
Salivary glands
Muscle
bone
Rep organs
Skin+Fur
Carcass
Biodistribution of [18F]-Al(OH)3 after i.v. injection
Standardized uptake values (SUV)
1.2
1
0.8
0.6
0.4
0.2
0
Blood
Thyroid
Stomach
Small Intestines
Large Intestines
Spleen
Liver
Kidneys
Heart
Lungs
Bladder
Salivary glands
Muscle
Urine
Bone